PHYSICAL REVIEW E **74**, 045603(R) (2006)

Spatial wave intensity correlations in quasi-one-dimensional wires

Gabriel Cwilich,[1] Luis S. Froufe-Pérez,[2] and Juan José Sáenz[2]
[1]*Department of Physics, Yeshiva University, 500 W 185th Street, New York, New York 10033, USA*
[2]*Departamento de Física de la Materia Condensada and Instituto "Nicolás Cabrera," Universidad Autónoma de Madrid, 28049 Madrid, Spain*

(Received 5 September 2005; revised manuscript received 23 July 2006; published 26 October 2006)

Spatial intensity correlations between waves transmitted through random media are analyzed within the framework of the random matrix theory of transport. Assuming that the statistical distribution of transfer matrices is isotropic, we found that the spatial correlation function can be expressed as the sum of three terms, with distinctive spatial dependences. This result coincides with the one obtained in the diffusive regime from perturbative calculations, but holds all the way from quasiballistic transport to localization. While correlations are positive in the diffusive regime, we predict a transition to *negative* correlations as the length of the system decreases.

DOI: 10.1103/PhysRevE.74.045603 PACS number(s): 42.25.Dd, 05.40.−a, 72.15.Rn

When a wave propagates coherently through a random medium important correlations emerge between the different propagating paths, which manifest themselves as correlations in the intensity speckle pattern. In contrast with the short range correlations characteristic of chaotic light [1], temporal, angular, and frequency [2,3,5,4,6–10] long range (C_2) and infinite range (C_3) correlations have been the subject of great interest over the last decade. Recently, the direct observation of spatial correlations in the intensity speckle pattern [11,12] and in the polarization [13] of electromagnetic waves transmitted through a random medium has renewed the interest in this problem [14].

One of the theoretical approaches followed to study this problem involved a microscopic diagrammatic calculation [4–6]. This was also the approach in the recent work that showed that the spatial correlation function of the normalized intensity can be expressed as the sum of three terms, which differ in their spatial dependence [11], and in the work finding an equivalent structure for the correlations in the polarized radiation [13]. However, the application of these approaches is strictly limited to the diffusive regime where the length of the disordered region L is much larger than the transport mean free path ℓ but still much smaller than the localization length ξ (i.e., $\ell \ll L \ll \xi$). Our main goal here is to extend these results to the quasiballistic and the localized regime.

An alternative approach, macroscopic in nature, has been applied successfully to study angular correlations in random media [7–10]; it considers the correlations between the transport coefficients in the scattering matrix describing the system in the framework of random matrix theory (RMT) [8,15,16]. Most of the work based on RMT has been focused on the study of angular or channel-channel correlations. It is the purpose of this work to apply the RMT approach to study the spatial intensity correlation functions. In analogy with angular correlations, we show that the assumption of isotropy of the transfer matrix determines the structure of the spatial correlations of the normalized intensity. Our result, which coincides with the one obtained from microscopic perturbative calculations (in the diffusive regime) [11] is not perturbative and holds all the way from quasiballistic transport to localization. Only the specific values of the three coefficients (C_1, C_2, and C_3) depend on the transport regime. These values, obtained from the Monte Carlo solution of the Dorokhov, Mello, Pereyra, and Kumar (DMPK) [15,17] scaling equation, are in full agreement with microscopic numerical calculations of bulk disordered wires. While long range correlations are positive in the diffusive regime, we predict a transition to *negative* values for both angular and spatial correlations when L is smaller that $\approx 2\ell$. Only when $L \approx 2\ell$ do the long range correlations disappear and the statistical properties of the light emerging from the random media are similar to those of a chaotic source. Although these results refer to classical correlations, they can also be relevant in the context of quantum correlation imaging [18] and quantum coherence [1] in random media.

We will consider a wave propagating in the z-direction in a constrained geometry (see the inset of Fig. 1). The eigenfunctions of the cavity (in the absence of disorder) separate into a longitudinal and a transverse part,

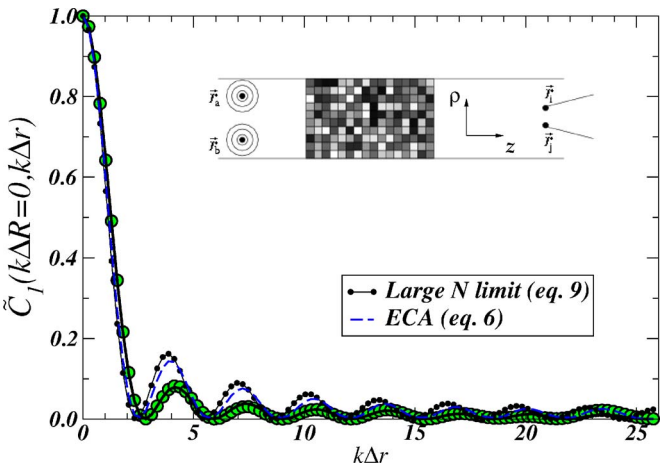

FIG. 1. (Color online) Square of the field correlation function for a single source as a function of the distance between detectors for a 2D waveguide. Circles correspond to microscopic numerical calculations (for $N=20$ and $g=1.12$) based on the model system sketched in the inset. The continuous line is the result of Eqs. (4) and (5) with $\langle T_{aj} \rangle$ obtained from the numerical calculations.

$$\phi_n^{\pm}(\mathbf{r}) = \frac{1}{\sqrt{k_n}}\psi_n(\rho)\exp\{\pm ik_n z\}, \tag{1}$$

where $\boldsymbol{\rho}$ are the transverse coordinates (we will only discuss the case of scalar waves in this work, neglecting polarization effects). The integer $n=1,2,\ldots,N$ labels the propagating modes, also referred to as scattering channels. Mode n has a real wave number $k_n=\sqrt{k^2-q_n^2}$, where k is the wave number of the incident radiation, and q_n is the momentum associated with the normalized transverse wave function $\psi_n(\boldsymbol{\rho})$. The normalization of the total wave function ϕ_n is chosen to carry unit current. Let us consider two point sources at $\mathbf{r}=\mathbf{r}_A$ and $\mathbf{r}=\mathbf{r}_B$ on the left-hand side of the system, and two detectors at $\mathbf{r}=\mathbf{r}_1$ and $\mathbf{r}=\mathbf{r}_2$ on the right side (as sketched in Fig. 1). For a point source at $\mathbf{r}=\mathbf{r}_A$ the incoming field from the left is proportional to the Green function of the clean waveguide,

$$G_0^+(\mathbf{r}_A,\mathbf{r}) = \frac{i}{2}\sum_a \phi_a^{+*}(\mathbf{r}_A)\phi_a^+(\mathbf{r});\ (z > z_A). \tag{2}$$

The field at a point $\mathbf{r}_1$ on the right side outside the system will be given by

$$E(A,1) = \sum_j \left\{ \sum_a t_{ja}c_a \right\} \phi_j^+(\mathbf{r}_1), \tag{3}$$

where $c_a \propto \phi_a^{+*}(\mathbf{r}_A)$. t_{ja} denote the transmitted amplitude in channel j when there is a unit flux incident from the left in channel a. The average intensity at that point is given by $\langle I(A,1)\rangle \equiv \langle |E(A,1)|^2\rangle$, where $\langle\cdots\rangle$ denotes disorder averaging (over the ensemble of samples). For a finite sample, the t_{ja}'s are assumed to have random phases with $\langle t_{ja}\rangle=0$ and $\langle t_{ja}t_{j'a'}^*\rangle = \langle T_{ja}\rangle\delta_{aa'}\delta_{jj'}$. The square of the field-field spatial correlation function can be written as

$$\tilde{C}_1(A,1;B,2) = \frac{|\langle E(A,1)E^*(B,2)\rangle|^2}{\langle I(A,1)\rangle\langle I(B,2)\rangle} \tag{4}$$

where

$$\begin{aligned}\langle E(A,1)E^*(B,2)\rangle &= \sum_{aa'jj'} c_a d_{a'}^* \phi_j^+(\mathbf{r}_1)\phi_{j'}^{+*}(\mathbf{r}_2)\langle t_{ja}t_{j'a'}^*\rangle \\ &= \sum_{aj} c_a d_a^* \phi_j^+(\mathbf{r}_1)\phi_j^{+*}(\mathbf{r}_2)\langle T_{ja}\rangle \end{aligned} \tag{5}$$

[with $d_a \propto \phi_a^+(\mathbf{r}_B)$]. The square of the field-field correlation function takes a simple form in the equivalent channel approximation (ECA): Assuming that $\langle T_{ja}\rangle = (1/N^2)\Sigma_{ja}\langle T_{ja}\rangle \equiv g/N^2$, Eq. (5) factorizes and

$$\tilde{C}_1(A,1;B,2) = |F(\mathbf{r}_A,\mathbf{r}_B)|^2 |F(\mathbf{r}_1,\mathbf{r}_2)|^2, \tag{6}$$

where $|F(1,2)|^2$ can be written in terms of the Green function (2):

$$|F(\mathbf{r}_1,\mathbf{r}_2)|^2 = \frac{|\mathrm{Im}\{G_0^+(\mathbf{r}_1,\mathbf{r}_2)\}|^2}{\mathrm{Im}\{G_0^+(\mathbf{r}_1,\mathbf{r}_1)\}\mathrm{Im}\{G_0^+(\mathbf{r}_2,\mathbf{r}_2)\}}. \tag{7}$$

In the large-N limit, the Green function of the clean waveguide tends to the free-space Green function, $\exp(ikr)/(4\pi r)$ in the case of a three-dimensional (3D) conductor, and we have

$$|F(\mathbf{r}_1,\mathbf{r}_2)|^2 \approx \left| \frac{\sin(k|\Delta\mathbf{r}_{12}|)}{k|\Delta\mathbf{r}_{12}|} \right|^2 \tag{8}$$

and analogous results hold in 2D with the "sinc" replaced by the Bessel function J_0:

$$|F(\mathbf{r}_1,\mathbf{r}_2)|^2 \approx J_0^2(k|\Delta\mathbf{r}_{12}|). \tag{9}$$

The behavior of the function $|F|^2$ vs $k\Delta r = k|x_1-x_2|$ is illustrated in Fig. 1. Black dots correspond to the large-N limit, Eq. (9). For a finite width, the field correlation function [Eq. (7)] strongly depends on the position of the detectors. Finite size effects can be minimized by using the experimental approach of Ref. [11]: we consider the average of $|F|^2$ when x_1 and x_2 are uniformly distributed over the interval $(W/10, W-W/10)$. As can be seen in Fig. 1, the averaged $|F|^2$ (dashed line) already presents the typical large-N behavior for the case of $N=20$.

The normalized spatial intensity correlation function can be defined as

$$C(A,1;B,2) \equiv \frac{\langle I(A,1)I(B,2)\rangle}{\langle I(A,1)\rangle\langle I(B,2)\rangle} - 1, \tag{10}$$

where the first term of the right-hand side is given by

$$\begin{aligned}\langle I(A,1)I(B,2)\rangle = \sum_{aa'bb'}\sum_{ii'jj'} \{(c_a c_{a'}^* d_b d_{b'}^*) \\ \times [\phi_j^+(\mathbf{r}_1)\phi_{j'}^{+*}(\mathbf{r}_1)\phi_i^+(\mathbf{r}_2)\phi_{i'}^{+*}(\mathbf{r}_2)] \\ \times \langle t_{ja}t_{j'a'}^* t_{ib}t_{i'b'}^*\rangle\}. \end{aligned} \tag{11}$$

In contrast with field-field correlations, the calculation of the averages presents subtle properties directly related to the symmetry properties of the scattering $\mathbf{S}$ matrix: flux conservation and reciprocity imply that $\mathbf{S}$ is unitary and symmetric. $\mathbf{S}$ admits a polar decomposition [15,16]:

$$\mathbf{S} = \begin{pmatrix} \mathbf{u}^{(1)} & 0 \\ 0 & \mathbf{u}^{(2)} \end{pmatrix} \begin{pmatrix} -\sqrt{1-\mathcal{T}} & \sqrt{\mathcal{T}} \\ \sqrt{\mathcal{T}} & \sqrt{1-\mathcal{T}} \end{pmatrix} \begin{pmatrix} \mathbf{u}^{(1)\mathsf{T}} & 0 \\ 0 & \mathbf{u}^{(2)\mathsf{T}} \end{pmatrix},$$

where $\mathbf{u}^{(i)}$ are unitary matrices and $\mathcal{T}=\mathrm{diag}(\mathcal{T}_1,\mathcal{T}_2,\ldots,\mathcal{T}_N)$ is a $N\times N$ diagonal matrix with the transmission eigenvalues on the diagonal. The transmission amplitudes can be written as

$$t_{ja} = \sum_n u_{jn}^{(2)}(\sqrt{\mathcal{T}_n})u_{an}^{(1)}. \tag{12}$$

One of the key assumptions in the macroscopic approach is the hypothesis of *isotropy* [8,15,16]. Under this hypothesis the statistical distribution of the transmission eigenvalues $\{\mathcal{T}_n\}$ is independent of the unitary matrices $\mathbf{u}^{(i)}$, and the calculation of the statistical averages in Eq. (11) factorizes. Moreover, $\mathbf{u}^{(1)}$ and $\mathbf{u}^{(2)}$ are statistically independent from each other, each being distributed according to the invariant measure of the unitary group. By using the averages over the unitary group $\langle (u_{jn})(u_{j'n'})^*\rangle$ and $\langle (u_{jn}u_{im})(u_{j'n'}u_{i'm'})^*\rangle$

(evaluated by Mello in Ref. [19]), after some algebra, we find

$$\langle t_{ja} t^*_{j'a'} \rangle = \frac{1}{N^2} \langle T \rangle \delta_{jj'} \delta_{aa'}, \tag{13}$$

$$\langle t_{ja} t^*_{j'a'} t_{ib} t^*_{i'b'} \rangle = [A_N \langle T^2 \rangle - B_N \langle T_2 \rangle](\delta_{ij'} \delta_{i'j} \delta_{ab'} \delta_{a'b} + \delta_{jj'} \delta_{ii'} \delta_{aa'} \delta_{bb'}) + [A_N \langle T_2 \rangle - B_N \langle T^2 \rangle] \times (\delta_{jj'} \delta_{ii'} \delta_{ab'} \delta_{a'b} + \delta_{ij'} \delta_{i'j} \delta_{aa'} \delta_{bb'}) \tag{14}$$

introducing the notation $g = \langle T \rangle \equiv \Sigma_n \langle \mathcal{T}_n \rangle$, $\mathrm{var}\{g\} \equiv \langle T^2 \rangle - \langle T \rangle^2$, $\langle T_2 \rangle \equiv \Sigma_n \langle \mathcal{T}_n^2 \rangle$, and the coefficients A_N and B_N given by

$$A_N = \frac{N^2+1}{N^2} \frac{1}{(N^2-1)^2}; \quad B_N = \frac{2}{N} \frac{1}{(N^2-1)^2}.$$

From Eq. (14), and taking $i=i'$, $j=j'$, $a=a'$, $b=b'$, we easily recover the well-known channel-channel correlation function C_{jaib} [7]

$$\frac{\langle T_{ja} T_{ib} \rangle}{\langle T_{ja} \rangle \langle T_{ib} \rangle} - 1 = C_1(\delta_{ij}\delta_{ab}) + C_2(\delta_{ab} + \delta_{ij}) + C_3, \tag{15}$$

where

$$C_1 \equiv \frac{N^4}{\langle T \rangle^2} [A_N \langle T^2 \rangle - B_N \langle T_2 \rangle], \tag{16}$$

$$C_2 \equiv \frac{N^4}{\langle T \rangle^2} [A_N \langle T_2 \rangle - B_N \langle T^2 \rangle], \tag{17}$$

$$C_3 \equiv C_1 - 1. \tag{18}$$

The angular correlation function has the same structure as the one found first by Feng *et al.* [6], the three coefficients C_1, C_2, and C_3 corresponding, respectively, to short, long, and infinite range correlations.

Substituting Eqs. (13) and (14) in Eqs. (5) and (11), we obtain the spatial intensity correlation function

$$C(\Delta \mathbf{r}_{ab}, \Delta \mathbf{r}_{12}) \equiv \frac{\langle I(a,1) I(b,2) \rangle}{\langle I(a,1) \rangle \langle I(b,2) \rangle} - 1 = [|F(\mathbf{r}_a, \mathbf{r}_b)|^2 |F(\mathbf{r}_1, \mathbf{r}_2)|^2] C_1 + [|F(\mathbf{r}_a, \mathbf{r}_b)|^2 + |F(\mathbf{r}_1, \mathbf{r}_2)|^2] C_2 + C_3, \tag{19}$$

where the correlation coefficients C_1, C_2, and C_3 are *exactly the same* as those appearing in Eq. (15). The structure of the spatial correlations is, then, equivalent to that obtained for channel correlations with the angular "δ_{ab}" functions replaced by the spatial functions $|F(a,b)|^2$ [Eq. (7)].

The spatial intensity-intensity correlation differs from the square of the field-field correlation, Eq. (6) (typical of chaotic waves). The behavior of the difference $[C(\Delta \mathbf{r}_{ab}, \Delta \mathbf{r}_{12}) - \tilde{C}_1(\Delta \mathbf{r}_{ab}, \Delta \mathbf{r}_{12})]$ is illustrated in Fig. 2 (for a 2D waveguide). For a single source and two detectors ($\Delta \mathbf{r}_{ab} = \Delta R = 0$ and $\Delta \mathbf{r}_{12} \equiv \Delta \mathbf{r}$), or vice versa, it is given by $\approx (C_2 + C_3)(1 + |J_0(k\Delta \mathbf{r})|^2)$ and approaches a constant as $\Delta \mathbf{r}$ increases. For large ΔR, the correlations as a function of $\Delta \mathbf{r}$

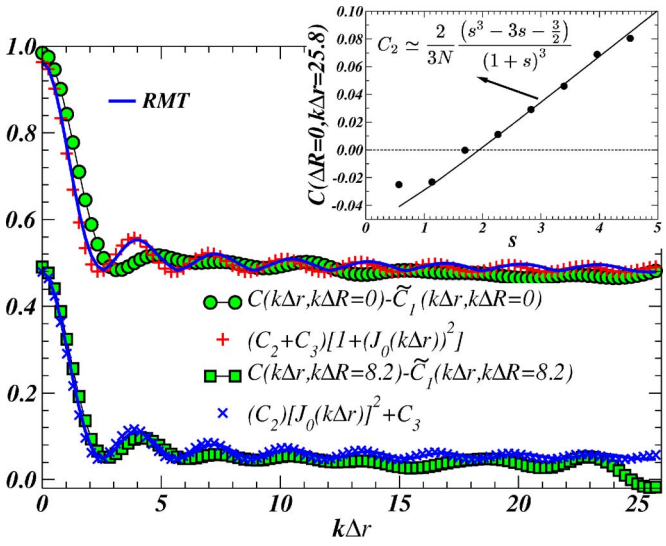

FIG. 2. (Color online) Plots of the intensity correlation function. Inset: Long range intensity correlations (C_2) as a function of the length $s = L/\ell$ of the system. Black dots are the results of numerical calculations.

behave as $\approx C_2[J_0(k\Delta \mathbf{r})]^2 + C_3$. These results are in qualitative agreement with the results of Ref. [11]. As a matter of fact, our expressions (19) and (7) [or Eq. (8) in the large-N limit] are consistent, after a slight reordering of the terms, with the expression (5) in reference [11]. The equivalence with polarization correlations [Eq. (2) of Ref. [13]] is also evident. However, while the diagrammatic expansions are strictly valid in the diffusive regime, our results *do not depend at all on the transport regime*, and are a direct consequence of the isotropy hypothesis. Only the relative *size* of C_1, C_2, and C_3 will depend on the length of the system L and

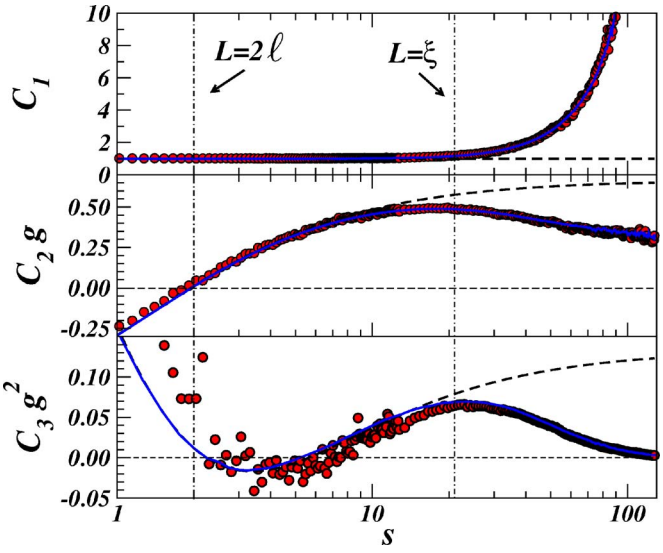

FIG. 3. (Color online) Correlation coefficients C_1, C_2, and C_3 as a function of the length $s = L/\ell$ of the system for $N=20$. Continuous lines are the results of the DMPK equation. The dashed line represents the perturbative $1/N$ expansion (after Ref. [10]). Circles are numerical results for the model system sketched in Fig. 1

the mean free path ℓ through the distribution of transmission eigenvalues $P(\{\mathcal{T}_n\},s)$, with $s=L/\ell$.

In the diffusive regime ($1 \ll g \ll N$), the correlation coefficients take the well-known values [6,7]: $C_1 \approx 1$, $gC_2 \approx 2/3$, and $g^2C_3 \approx 2/15$. We have obtained their dependence with the length of the system (summarized in Fig. 3 for $N=20$) by solving the DMPK equation using the Monte Carlo approach of Ref. [20]. For $L \gtrsim \xi$, $C_2 g$ and $C_3 g^2$ decrease although C_1, C_2, and C_3 themselves present an exponential growth with L in the localized regime. For $L \lesssim \xi$ (or $g \gtrsim 1$), the exact solution of the DMPK equation is well described by the known analytical results based on $1/N$ expansion [10] (dashed line in Fig. 3). In agreement with previous results on angular correlations [10], our work predicts a transition from positive to negative long range spatial correlations as the length of the system decreases.

In order to confirm the predictions of the macroscopic approach, we have performed extensive numerical calculations based on the simple two-dimensional (2D) model sketched in Fig. 1. For electromagnetic waves, we assume *s*-polarization with the electric vector parallel to the walls. The disordered region is divided in small rectangular regions of section $\delta_z \times \delta_x$. Within each slice the refraction index n_R has random values distributed uniformly in the interval $(1-\delta n_R,\ 1+\delta n_R)$. We take $\delta_x = W/10$, $\delta_z = W/20$, and $\delta n_R = 0.025$, for a 20-mode waveguide ($W/\lambda = 10.25$) as in Fig. 1. Transmission and reflection coefficients are exactly calculated by solving the 2D wave equation by mode matching at each δ_z-slice, together with a generalized scattering-matrix technique [21]. Figure 1 shows the behavior of the averaged field correlations (for $s=15$, $\langle g \rangle = 1.12$). The numerical intensity correlations are very close to the expected behavior (see Fig. 2) although they are not fully described by Eqs. (15) and (19) since transport is not fully isotropic. However, we can extract the correlation coefficients C_1, C_2, and C_3 from a least-squares fitting of spatial or angular numerical correlations with Eq. (19) or (15), respectively. In both cases, the obtained coefficients (circles in Fig. 3) are in full agreement with the predictions of the DMPK approach.

The predicted nontrivial dependence of the *spatial* intensity correlations with L/ℓ should be observable in actual microwave experiments [11] by changing either L or the frequency, filling the tube with samples having a strong dependence of ℓ with the frequency [22].

This work has been supported by the Spanish MCyT (Ref. No. BFM2003-01167) and the EU Integrated Project "Molecular Imaging" (LSHG-CT-2003-503259). One of us (G.C.) wants to acknowledge the support of the Condensed Matter Physics Dept. of the Universidad Autonoma de Madrid, where part of his work was performed.

[1] L. Mandel and E. Wolf, *Optical Coherence and Quantum Optics* (Cambridge Univ. Press, New York 1995); R. Loudon, *The Quantum Theory of Light* (Oxford Univ. Press, Oxford, 2000).
[2] *Waves and Imaging through Complex Media*, edited by P. Sebbah (Kluwer, Dordrecht, 2001).
[3] *Wave Scattering in Complex Media: From Theory to Applications*, edited by B. van Tiggelen and S. Skipetrov (Kluwer, Dordrecht, 2003).
[4] I. Freund, M. Rosenbluh, and S. Feng, Phys. Rev. Lett. **61**, 2328 (1988).
[5] M. J. Stephen and G. Cwilich, Phys. Rev. Lett. **59**, 285 (1987).
[6] S. Feng, C. Kane, P. A. Lee, and A. D. Stone, Phys. Rev. Lett. **61**, 834 (1988); R. Brekovits and S. Feng, Phys. Rep. **238**, 135 (1994).
[7] P. A. Mello, E. Akkermans, and B. Shapiro, Phys. Rev. Lett. **61**, 459 (1988).
[8] P. A. Mello and A. D. Stone, Phys. Rev. B **44**, 3559 (1991).
[9] E. Bascones, M. J. Calderon, D. Castelo, T. Lopez, and J. J. Saenz, Phys. Rev. B **55**, R11911 (1997).
[10] A. García-Martín, F. Scheffold, M. Nieto-Vesperinas, and J. J. Saenz, Phys. Rev. Lett. **88**, 143901 (2002); J. J. Sáenz, L. S. Froufe-Pérez, and A. García-Martín, in Ref. [3], p. 175.
[11] P. Sebbah, B. Hu, A. Z. Genack, R. Prini, and B. Shapiro, Phys. Rev. Lett. **88**, 123901 (2002).
[12] V. Emiliani *et al.*, Phys. Rev. Lett. **90**, 250801 (2003).
[13] A. A. Chabanov, N. P. Tregoures, B. A. van Tiggeler, and A. Z. Genack, Phys. Rev. Lett. **92**, 173901 (2004).
[14] Y. H. Kim, U. Kuhl, H. J. Stockmann, and P. W. Brouwer, Phys. Rev. Lett. **94**, 036804 (2005); S. E. Skipetrov, *ibid.* **93**, 233901 (2004); A. A. Chabanov, B. Hu, and A. Z. Genack, *ibid.* **93**, 123901 (2004); V. M. Apalkov, M. E. Raikh, and B. Shapiro, *ibid.* **92**, 253902 (2004).
[15] P. A. Mello, P. Pereyra, and N. Kumar, Ann. Phys. (N.Y.) **181**, 290 (1988).
[16] C. W. J. Beenakker, Rev. Mod. Phys. **69**, 731 (1997).
[17] O. N. Dorokhov, Solid State Commun. **51**, 381 (1984).
[18] A. Gatti, E. Brambilla, M. Bache, and L. A. Lugiato, Phys. Rev. A **70**, 013802 (2004); P. Lodahl, A. P. Mosk, and A. Lagendijk, Phys. Rev. Lett. **95**, 173901 (2005); G. Scarcelli, V. Berardi, and Y. Shih, *ibid.* **96**, 063602 (2006).
[19] P. A. Mello, J. Phys. A **23**, 4061 (1990).
[20] L. S. Froufe-Pérez, P. Garcia-Mochales, P. A. Serena, P. A. Mello, and J. J. Saenz, Phys. Rev. Lett. **89**, 246403 (2002).
[21] J. A. Torres and J. J. Sáenz, Jpn. J. Appl. Phys., Part 1 **73**, 2182 (2004).
[22] A. A. Chabanov, M. Stoytchev, and A. Z. Genack, Nature (London) **404**, 850 (2000).